PHILOSOPHICAL TRANSACTIONS A

royalsocietypublishing.org/rsta

CC BY

Review

Cite this article: Vallis G, Matilsky L, Nicholas Q. 2026 Jets and superrotation in deep and shallow planetary atmospheres. *Phil. Trans. R. Soc. A* **384**: 20250135.
https://doi.org/10.1098/rsta.2025.0135

Received: 15 November 2025
Accepted: 27 March 2026

One contribution of 14 to a theme issue 'Anti-diffusive transport and layering: from sub-cellular to astrophysical scales'.

Subject Areas:
extrasolar planets, atmospheric science, meteorology, astrophysics

Keywords:
planetary atmospheres, jets, superrotation, GFD

Author for correspondence:
Geoffrey Vallis
e-mail: g.vallis@exeter.ac.uk

Jets and superrotation in deep and shallow planetary atmospheres

Geoffrey Vallis[1], Loren Matilsky[2] and Quentin Nicholas[3]

[1]Mathematics and Statistics, University of Exeter, Exeter, UK
[2]Applied Mathematics, UCSC, Santa Cruz, CA, USA
[3]ETH Zurich, Zürich, ZH, Switzerland

GV, 0000-0002-5971-8995

Zonal flows in planetary atmospheres are ubiquitous, and nearly all the planets in the Solar System have flows that are zonally rather than meridionally aligned. *Jets*, which are essentially concentrated streams of fluid that are distinct from a more quiescent background, are less common but can also be found in both deep and shallow atmospheres. Superrotation, which in most circumstances simply means prograde motion (relative to the planetary rotation) at the equator, is less common but can be found in both deep and shallow planetary atmospheres, and in both quickly and slowly rotating atmospheres: Jupiter, Saturn, Venus and Titan all have superrotating atmospheres. Jets, especially superrotating jets, imply some form of 'antidiffusion' of momentum, meaning that momentum (or angular momentum) must be transported upgradient. This article discusses some of the mechanisms that give rise to jets and superrotation in both deep and shallow planetary atmospheres, on both slow and fast rotators, contrasting and comparing the processes involved. Topics discussed include the roles of convection in deep atmospheres, geometric and topographic β-effects, potential-vorticity homogenization, wave–mean-flow interaction and tidal locking in exoplanets.

This article is part of the theme issue 'Anti-diffusive transport and layering: from sub-cellular to astrophysical scales'.

© 2026 The Authors. Published by the Royal Society under the terms of the Creative Commons Attribution License http://creativecommons.org/licenses/by/4.0/, which permits unrestricted use, provided the original author and source are credited.

THE ROYAL SOCIETY PUBLISHING

Downloaded from royalsocietypublishing.org/rsta/article-pdf/doi/10.1098/rsta.2025.0135/6176045/rsta.2025.0135.pdf
by ETH Zurich user
on 23 November 2026

1. Introduction

Zonal flows are a common feature in planetary atmospheres, at least in our Solar System and most likely also in exoplanets. The underlying reason for this is simple: rotation inhibits strong meridional flows on the surface of a spherical body because, if a parcel of fluid were to move any distance meridionally, the conservation of angular momentum would lead to strong zonal flows. Those zonal flows might be unstable or be associated with strong meridional temperature gradients, but in any case the zonal flows would soon be stronger and more persistent than the meridional flows. A similar argument using the vorticity equation on the β-plane implies that the meridional velocity, v, must be small if β, the latitudinal gradient of the Coriolis parameter f, is large. Put simply, the barotropic vorticity equation has the form $\beta v =$'other terms', and if β increases while the other terms stay approximately the same, then v must diminish but u, the zonal velocity, need not. (On the sphere, $f = 2\Omega \sin\theta$, where Ω is the planetary rotation rate and θ is latitude, and $\beta = a^{-1}\partial f/\partial\theta = 2a^{-1}\Omega\cos\theta$. On the commonly used β-plane, $f = f_0 + \beta y$, where f_0 and β are constants and y is the distance in the meridional direction.)

Such simple arguments cannot explain how *jets* form or, in particular, how superrotation forms. Jets may be regarded as concentrated streams that are distinct from a more quiescent background. Superrotation is a prograde flow (relative to the planetary rotation) for which a ring of fluid going round the planet has an average angular momentum exceeding that of the planet itself at the equator at some reference level, commonly taken to be at the solid surface for terrestrial planets and at some reference pressure in the case of gas or ice giants. (This can lead to some arbitrariness, especially if one seeks to extend the definition to stars.) In nearly all cases, superrotation is associated with prograde motion at the equator; if the superrotation were only at higher latitudes, the flow would be inertially unstable.

Jets and superrotation both require some form of upgradient transfer of momentum: diffusion will seek to dissipate any extremum of velocity, and thus, there must be some other process to counter that effect. Superrotation has been observed on both deep and shallow atmospheres. The former are often associated with giant planets, and the atmospheres of both Jupiter and Saturn superrotate, whereas those of Uranus and Neptune do not. (Henceforth, we may say 'the planet superrotates', and it should be understood that it is the atmosphere that is superrotating.) Shallow atmospheres are typical of terrestrial atmospheres, and in the Solar System both Venus and Titan superrotate, whereas on average Earth does not, although it does from time to time, sometimes associated with the quasi-biennial oscillation. Outside the Solar System, there is compelling evidence, albeit somewhat indirect, that some tidally locked planets—both hot Jupiters and super-Earths—superrotate.

It is the purpose of this article to describe and discuss the various mechanisms that might give rise to jets and superrotation in various forms of planetary atmospheres. It is not a literature review; rather, it is a synthesis and focused discussion of the various mechanisms involved in deep and shallow atmospheres on both slowly and quickly rotating planets. We seek to draw attention to commonalities and differences, indicating how robust or delicate various mechanisms may be, and what the remaining problems and uncertainties are. We give few observational examples: a description of the observations is not our goal and would require an article unto itself. A number of review articles on related topics have previously appeared that cover observations, models or particular cases in more detail, for example, Imamura *et al.* [1], Read & Lebonnois [2], Pierrehumbert & Hammond [3], Read [4] and some of the articles in the collection by Galperin & Read [5]. References to the primary literature are given in the main body of the paper. The first couple of sections below reprise material that can be found in standard texts but which is included because it is foundational and keeps the discussion self-contained.

2. Jets and Rossby waves

The production of jets by the effects of Rossby waves on the mean flow is a well-known mechanism that is responsible for the production of the 'eddy-driven' zonal jet in Earth's

Downloaded from royalsocietypublishing.org/rsta/article-pdf/doi/10.1098/rsta.2025.0135/6176045/rsta.2025.0135.pdf
by ETH Zurich user
on 23 November 2026

mid-latitudes; it likely occurs on other shallow atmospheres, and perhaps in a different form on deep atmospheres.

(a) An eddy-driven jet

A familiar, and probably the best understood, mechanism involving Rossby waves involves the localized generation and meridional propagation of such waves, leading to an eastward jet in the region of the wave generation [6–8]. Suppose that Rossby waves are excited within some compact range of latitudes and that the dissipation mechanisms or refraction are insufficient to prevent the meridional propagation of the waves away from the source region. In incompressible two-dimensional flow on the β-plane, the familiar dispersion relation for Rossby waves is

$$\omega = Uk - \frac{\beta k}{k^2 + l^2}, \tag{2.1}$$

where ω is the frequency, k and l are zonal and meridional wavenumbers, respectively, U is the (here assumed unsheared) constant background zonal flow and β is a constant, as introduced earlier.

The meridional component of group velocity is

$$c_g^y = \frac{\partial \omega}{\partial l} = \frac{2\beta k l}{(k^2 + l^2)^2}\,. \tag{2.2}$$

This must be directed away from the source region, since energy is carried with the group velocity. For incompressible flow, the velocity components in the zonal (x) and meridional (y) directions associated with the Rossby waves are

$$u' = -\mathrm{Re}\, C\, \mathrm{i} l \mathrm{e}^{\mathrm{i}(kx+ly-\omega t)} \qquad \text{and} \qquad v' = \mathrm{Re}\, C\, \mathrm{i} k \mathrm{e}^{\mathrm{i}(kx+ly-\omega t)}, \tag{2.3a,b}$$

where C is the complex amplitude of the stream function of the waves. The momentum flux (taking density equal to one) carried by the waves is therefore

$$\overline{u'v'} = -\frac{1}{2}|C|^2 kl, \tag{2.4}$$

with the overbar denoting a zonal average and primes a deviation from the average. The momentum flux associated with the Rossby waves thus has the *opposite* sign to that of the group velocity; thus, if Rossby waves travel away from the source region, momentum fluxes towards the source region, converging in that region and generating a prograde flow, as in figure 1. The mechanism relies in a fundamental way on the presence of a potential vorticity gradient that allows Rossby waves to propagate.

The mechanism may also be succinctly described by the transformed Eulerian mean formalism; this can lead to some advantages in more complicated situations, for example, stratified flow involving buoyancy fluxes in which use of the potential vorticity and/or Eliassen–Palm fluxes can be helpful. In any case, it is the presence of a potential vorticity gradient allowing for the propagation of Rossby-like waves that is essential, and this can be produced by differential rotation, the effects of stratification or topographic effects; in all cases, the essential mechanism is that above or variations on that effect [9].

It is this mechanism that produces an eastward, largely barotropic flow and an associated eastward surface flow, in Earth's mid-latitudes, sometimes called the eddy-driven jet. This jet should be mechanistically distinguished from the general eastward thermal wind that is associated with the pole–equator temperature gradient, although this too produces a prograde flow when high latitudes are cooler than low ones [10,11]. On Earth, there is subtropical jet at the edge of the Hadley Cell that has very little eddy forcing, being mainly comprised of a vertically sheared zonal flow in thermal wind balance. By contrast, the mid-latitude jet has an eddy-driven component with a

Downloaded from royalsocietypublishing.org/rsta/article-pdf/doi/10.1098/rsta.2025.0135/6176045/rsta.2025.0135.pdf
by ETH Zurich user
on 23 November 2026

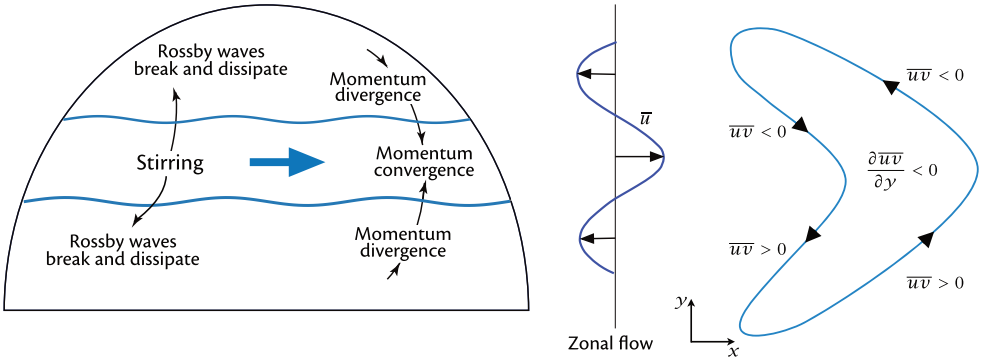

Figure 1. Generation of zonal flow on a rotating sphere or β-plane. Stirring in mid-latitudes (for example by baroclinic eddies) generates Rossby waves that propagate away. Momentum converges in the region of stirring, producing eastward flow there and weaker westward flow on its flanks. The right-hand plot shows the momentum transport in physical space produced by the boomerang-shaped eddies produced by the waves. Adapted from Vallis [9].

strong barotropic component. This jet is superimposed on the thermal wind, and the subtropical and eddy-driven jets are often merged and observationally barely distinguishable from each other even if the mechanisms producing them are distinct. In the upper troposphere on Earth, the broad eastward flow that arises from the thermal wind balance is at least as large as the eddy-driven component, but this is not obviously the case on the giant planets.

(b) Multiple jets on the β-plane and sphere

Multiple, alternating east–west, jets can also form on the β-plane or on the surface of a rotating sphere. However, the description of their formation commonly differs from that above, being couched in the language of two-dimensional (or geostrophic) turbulence in which the governing equation is the barotropic vorticity equation

$$\frac{\partial \zeta}{\partial t} + J(\psi, \zeta) + \beta \frac{\partial \psi}{\partial x} = -r\zeta + \nu \nabla^2 \zeta + F. \tag{2.5}$$

Here, ψ is the stream function of the flow (such that $u = -\partial_y \psi v = \partial_x \psi$), $\zeta = \nabla^2 \psi$ is the relative vorticity, J is the Jacobian ($J(\psi, \zeta) = \partial_x \psi \partial_y \zeta - \partial_y \psi \partial_x \zeta$), r and ν are linear drag and viscous coefficients (respectively) and F is the imposed forcing, often supposed to be at some small scale. Energy is then generated at small scales (where the nonlinear terms dominate) and is transferred by some form of inverse cascade to large scales where flow becomes more linear and Rossby waves dominate, leading to jet formation. A scaling for the crossover scale, simply based on dimensional arguments, is

$$L_R = \left(\frac{U}{\beta}\right)^{1/2}, \tag{2.6}$$

where U is some representative fluid speed of the eddying flow, and this scale is commonly called, and taken to be the definition of, the Rhines scale [12]. Because the estimate is obtained by comparing a turbulence speed to a Rossby wave speed, U is most naturally thought of as a root-mean-square (rms) velocity—ideally at the crossover scale itself—and not the velocity of the jet. In some circumstances, the mean zonal velocity itself might be used as a rough measure of U but this is not generally appropriate.

Equation (2.6) is not a prediction for the crossover scale, since U is not known *a priori* nor is it always easily measured. Instead, one may take the energy injection rate, ϵ (which is equal to the cascade rate), to be known, for this is an external parameter. In numerical simulations, one

Downloaded from royalsocietypublishing.org/rsta/article-pdf/doi/10.1098/rsta.2025.0135/6176045/rsta.2025.0135.pdf
by ETH Zurich user
on 23 November 2026

can control the value of ϵ, and in planetary atmospheres one may be able to determine it if the internal heat flux is known and/or from the radiation budget at the top of the atmosphere. Given ϵ, a standard turbulence-based scaling connecting the velocity U with scale L is $\epsilon \sim (U^3/L)$. Using this in equation (2.6) gives the β-scale [13]

$$L_\beta = \left(\frac{\epsilon}{\beta^3}\right)^{1/5}. \tag{2.7}$$

This scale is not the scale at which the inverse cascade ceases; rather, it is the scale at which the flow becomes more zonally oriented through the action of Rossby waves that allow the energy to proceed to large scales only if it becomes zonally elongated, and so become jet-like [13]. (Wave–wave interactions among Rossby waves themselves also have a tendency to produce zonal flows [12,14].) The inverse cascade finally halts owing to the effect of linear drag, and if the rms velocity at the halting scale is given by $U \sim (\epsilon/r)^{1/2}$, then, using this estimate in equation (2.6), we obtain the scale

$$L_{\beta r} = \left(\frac{\epsilon}{r\beta^2}\right)^{1/4}. \tag{2.8}$$

This scale is not the only one that can be constructed form β, ϵ and r, but it is physically motivated, and for small friction $L_\beta < L_{\beta r}$. The length scales given by equations (2.7) and (2.8) may be put in the form of $(U/\beta)^{1/2}$, with particular choices of U, and in that sense are Rhines scales; however, for clarity, they are often referred to as the β-scale and β-r-scale, respectively. The scale around $L_{\beta r}$, if larger than L_β, does seem to be the meridional scale at which zonal jets form in numerical simulations [15], and so is a measure of their width. The region between L_β and $L_{\beta r}$ (when the latter is larger) is known as the zonostrophic regime, and scaling arguments suggest that the kinetic energy spectrum in that region is anisotropic and should follow $E(k) = C_z\beta^2 k^{-5}$ for small zonal wavenumber, where k is the total wavenumber and C_z is some constant [16].

The case when r tends to zero is an interesting one, whether or not β is non-zero. If the Laplacian viscosity is also small, then, in the barotropic (two-dimensional) case, there is no mechanism to halt the inverse transfer of energy. The scale of motion—whether zonal flows or vortices—will continue to grow, limited only by the size of the domain, with the kinetic energy continuing to pile up at that scale [17]. A Laplacian viscosity cannot prevent this unless it is large enough to operate across all scales, in which case the flow is no longer turbulent. In a baroclinic fluid (and so in planetary atmospheres), there is another escape route for the kinetic energy, namely conversion to baroclinic energy at large scales; the energy there can be thermally damped, and this may allow the fluid to equilibrate even with zero drag [18]. This route may be important in giant planets although it has yet to be fully explored.

The mechanism of multiple jet formation should not be regarded as wholly different from that described in §2a, in which each prograde jet is still proximately produced by eddy momentum flux convergence from Rossby wave propagation. However, in the homogeneous, multi-jet case, the position of each jet is more arbitrary and not necessarily determined by the position of some localized external forcing.

(c) Potential vorticity homogenization and staircases

We may write equation (2.5) in the equivalent form

$$\frac{\mathrm{D}q}{\mathrm{D}t} = F - D, \tag{2.9}$$

where $q = \zeta + \beta y$, and F and D represent forcing and dissipation, respectively; evidently, the above equation has the same form as that governing a passive scalar. If the flow is turbulent but the forcing and dissipation are weak, there will be a tendency for the potential vorticity to homogenize

Downloaded from royalsocietypublishing.org/rsta/article-pdf/doi/10.1098/rsta.2025.0135/6176045/rsta.2025.0135.pdf
by ETH Zurich user
on 23 November 2026

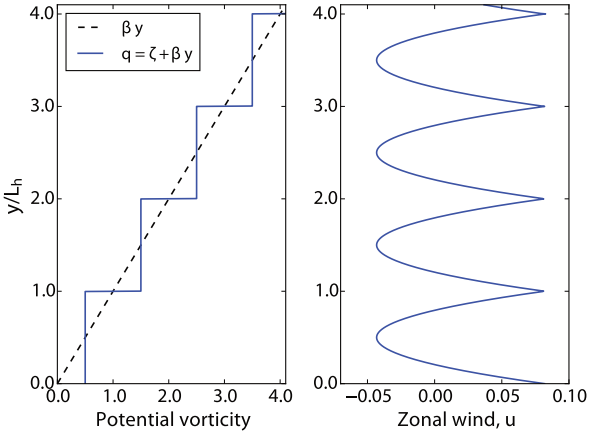

Figure 2. An idealized potential vorticity staircase. The left panel shows homogeneous regions of potential vorticity separated by jumps, with the homogenization occurring over a scale $(U/\beta)^{1/2}$. The right-hand panel shows the corresponding zonal flow. Adapted from Vallis [11].

[19], with gradients of potential vorticity being expelled to a boundary. (This result is a variation on the well-known Prandtl–Batchelor effect: vorticity in a region surrounded by a closed streamline must be constant.) However, there may be insufficient energy for the entire domain to become homogenized, in which case regions may become homogeneous with rapid gradients between them, and in a zonally re-entrant domain, a potential vorticity staircase may form (figure 2) with most of the kinetic energy in the zonal flow. Marcus [20] and Marcus & Shetty [21] proposed the relevance of this mechanism to jet formation in planetary atmospheres, and others have explored the mechanism more generally, e.g. [22,23]. A closely related mechanism producing staircase-like structures of density in stratified flow was previously identified in an oceanographic context by Phillips [24] and Posmentier [25], and the analogy to potential vorticity mixing and inverse cascade was further cemented by Cabanes *et al.* [26] using the sorting algorithm of Thorpe [27]. Earlier observations of layering were actually made by Tait & Howe [28], and thermohaline staircases in stratified fluids are now fairly commonly observed.

(d) Deep and shallow atmospheres

The mechanisms of jet formation described above are two-dimensional; that is, they can be described by equations in which the fields vary only in latitude and longitude. In a shallow atmosphere in which the atmospheric depth is much less than the planetary radius, which is typical of the terrestrial planets in the Solar System, quasi-two-dimensionality can be regarded as a reasonable approximation; indeed, the quasi-geostrophic equations (which do allow for vertical structure) exhibit similar behaviour to the purely two-dimensional equations because they have a conserved potential vorticity that is more-or-less a Laplacian of the stream function, an inverse cascade of energy that can be diverted by a β-effect and a forward cascade of enstrophy [29,30]. However, the gas giants do not have shallow atmospheres; the planets are themselves fluids, albeit not always gaseous and with densities that increase enormously with depth. That said, there are two effects that may make the atmospheres behave in a quasi-two dimensional fashion, as follows.

The first is simply that the upper atmospheres of the gas giants (the 'weather layers') are, at least to some degree, stably stratified (figure 3). Although the most direct evidence for this comes from a single location using the Galileo probe, temperature profiles obtained from Voyager occultation measurements [31,32] give a qualitatively consistent view. Stratification may arise through radiative effects (with radiation becoming more efficient than convection in transporting energy upward in the weather layers) and/or through moist convection; which of the two is the

Downloaded from royalsocietypublishing.org/rsta/article-pdf/doi/10.1098/rsta.2025.0135/6176045/rsta.2025.0135.pdf
by ETH Zurich user
on 23 November 2026

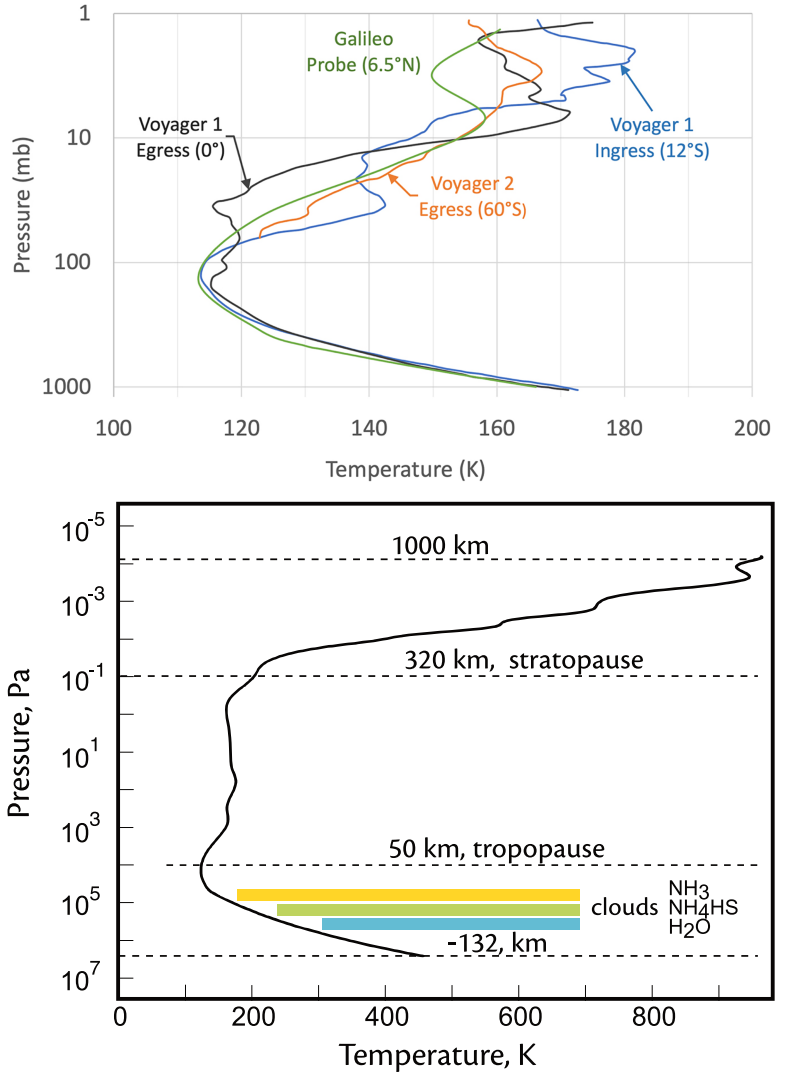

Figure 3. Temperature in Jupiter's upper atmosphere. Panel (a), from Gupta *et al.* [31], uses data from Voyager radio measurements. Panel (b) is adapted from Ruslik0 at en.wikipedia using data from the Galileo probe, with heights measured from the 10^5 Pa (1000 mb) level.

dominant mechanism (if there is one) in the Solar System gas giants is not known. Stratification inhibits vertical motion and leads to a more two-dimensional flow, and if the Rossby number is low, the combined effects lead to the quasi-geostrophic equations.

The second reason is that, even if the flow is deep, the presence of rapid rotation organizes the flow into columnar structures that are largely invariant along the axis of rotation—a manifestation of the Taylor–Proudman effect. This effect has manifestations even when the flow is convecting, enabling the flow to be described by a set of quasi-geostrophic-like equations [33–35] that have similar properties to those of the more familiar quasi-geostrophic equations for shallow, stratified flow.

The above two effects have led to competing views of the origin of the jets observed on the giant planets in the Solar System. One mechanism emphasizes the weather layer, in which geostrophic turbulence on the β-plane can lead to jet formation through the mechanisms described in §2a,b. A mechanism for superrotation is less obvious in this context, although if Rossby waves can be

Downloaded from royalsocietypublishing.org/rsta/article-pdf/doi/10.1098/rsta.2025.0135/6176045/rsta.2025.0135.pdf
by ETH Zurich user
on 23 November 2026

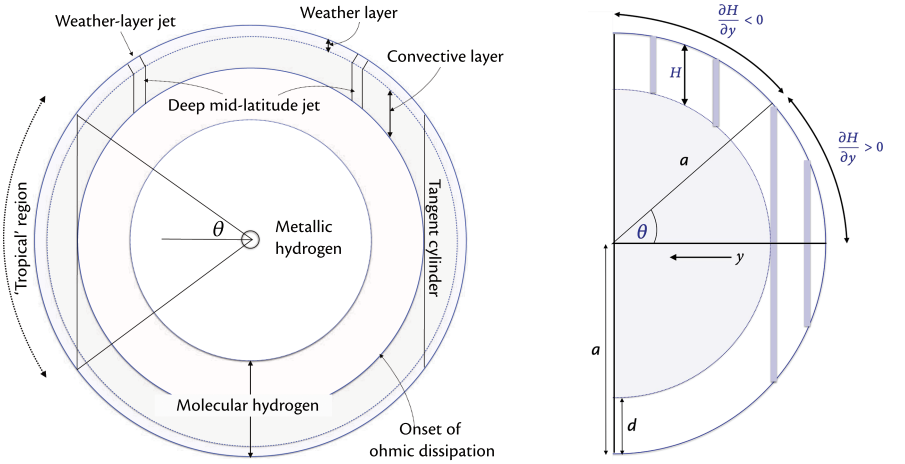

Figure 4. Idealized structure and geometry of a giant planet, such as Jupiter or Saturn. The right-hand panel shows how the thickness of the convecting shell changes with distance from the rotation axis, and so with latitude. Adapted from Vallis [11].

generated at the equator and propagate poleward in each hemisphere, then equatorial superrotation can arise [36,37]. By contrast, Busse suggested that the jets on Jupiter are a manifestation of deep convection, with the role of any weather layer being secondary. The convective cells become aligned with the axis of rotation, and a topographic β-effect arises because the depth of the shell in the direction of the axis of rotation varies with cylindrical distance from the axis of rotation, and so with latitude (figure 4). The flow can then take on a quasi-geostrophic form, and zonal jets can form. In the equatorial region, the variation of shell depth is the opposite to that in mid-latitudes (figure 4) so that an effective beta, now owing to variations in column depth, is *negative*. This gives a natural mechanism for the formation of superrotation, as we discuss in §3c.

Gravimetric observations from the Juno mission [38] indicate that the jets on Jupiter *do* extend into the atmosphere, probably to a depth of order 3000 km and likely with some variation in latitude, with those on Saturn extending still deeper [39]. The Jovian jets also appear to be aligned with the axis of rotation, at least below the weather layer. Although a few thousand kilometres is not deep compared to the radius of these planets, it is deep enough for a full treatment of the Coriolis effect to be needed. The low density of fluid in the weather layer and the relative shallowness of that layer (about 100 km) mean that the gravitational influence of the layer is too small for gravimetric observations to discern whether the flow is aligned along the axis of rotation or along radial lines in that region.

3. Mechanisms of superrotation

We now turn our attention to the mechanisms producing superrotation and, in particular, prograde motion at the equator.

(a) Constraints on superrotation and Hide's result

As noted, superrotation may be defined as the presence of a zonal flow whose average angular momentum around the planetary axis of rotation exceeds that of the planet itself at some reference level (e.g. the planet surface) at the equator. For simplicity, consider a shallow atmosphere (meaning that its depth is much smaller than the planetary radius, a) on a terrestrial planet. If the planet rotates at a rate Ω and the zonally averaged zonal velocity is $\overline{u}$, then the average angular

Downloaded from royalsocietypublishing.org/rsta/article-pdf/doi/10.1098/rsta.2025.0135/6176045/rsta.2025.0135.pdf
by ETH Zurich user
on 23 November 2026

momentum (per unit mass) of a ring of fluid at a given ϑ is given by

$$m = (\Omega a \cos\vartheta + \overline{u})\, a \cos\vartheta. \tag{3.1}$$

Let us suppose that $\overline{u} = 0$ at the equator (and thus $m(\vartheta = 0) = \Omega a^2$). A ring of air at the equator that moves poleward will, in the absence of viscosity, conserve its angular momentum so that at a latitude ϑ, its zonal wind is given by

$$\overline{u}(\vartheta) = \Omega a \frac{\sin^2\vartheta}{\cos\vartheta}. \tag{3.2}$$

If its velocity exceeds this, the ring will be superrotating. However, this is not easily achieved for the simple reason that m *is* conserved. That is, it obeys an equation of the form

$$\frac{\mathrm{D}m}{\mathrm{D}t} = D + E, \tag{3.3}$$

where D represents dissipation and E represents eddy effects. If $E = 0$ and D is the result of a Laplacian viscosity, and if the vertical scales are much smaller than the horizontal scales, then the viscous term is approximately $\nu\partial^2 m/\partial z^2$. In this case, dissipation can only dissipate extrema of angular momentum and no superrotation can form; this is essentially Hide's result [40]. (If viscosity is large enough to be dominant, the flow will tend towards three-dimensional solid-body rotation, but this is very unlikely if the dissipation arises from molecular effects.) However, superrotation can potentially form if the eddy terms, E, in equation (3.3) are non-zero, and Gierasch [41] suggested that vorticity mixing could give rise to superrotation. Various other forms of eddy viscosity and drag have also been proposed, e.g. [42]. In the next sections, we focus on the mechanisms of how eddies and/or wave–mean-flow interaction gives rise to superrotation.

(b) Superrotation in terrestrial atmospheres

Two rather different kinds of terrestrial planetary bodies are known to superrotate: slowly rotating planetary bodies (such as Venus and Titan) and some tidally locked planets. A robust mechanism producing superrotation on both classes of planets involves the interaction of Rossby and Kelvin waves, although the forcings of these waves differ considerably in the two cases. (Venus also has very long solar days, and tidal forcing is likely to be important; furthermore, many tidally locked planets are gas giants—effects we do not consider here.)

(i) Slow rotators

Numerical simulations suggest that superrotation on slowly rotating, shallow, planetary atmospheres (henceforth just 'slow rotators') is a robust effect, as illustrated in figure 5. One candidate mechanism for such superrotation is the production of Rossby waves in equatorial regions with subsequent meridional propagation, thus converging momentum to the equator in the manner similar to that described in §2a. However, on slow rotators, a mechanism for the generation of such Rossby waves is hard to envision, and in any case ageostrophic effects and Kelvin waves are likely to be important. Rather, the superrotation mechanism (at least that arising in numerical simulations) is that of an instability involving the interaction of off-equatorial Rossby waves and equatorial Kelvin waves. This 'RK (Rossby–Kelvin) instability' was identified by Iga & Matsuda [45] and further explored by Wang & Mitchell [46], and (now with hindsight) is recognized as the mechanism appearing in [47] and other simulations since, with Potter *et al.* [48] emphasizing the importance of Kelvin waves and Zurita-Gotor & Held [49] making explicit the connection to RK instability.

Kelvin waves typically have an eastward phase speed, whereas Rossby waves travel westward, and Kelvin waves decay away from the equator with Rossby waves more dominant at higher

Downloaded from royalsocietypublishing.org/rsta/article-pdf/doi/10.1098/rsta.2025.0135/6176045/rsta.2025.0135.pdf
by ETH Zurich user
on 23 November 2026

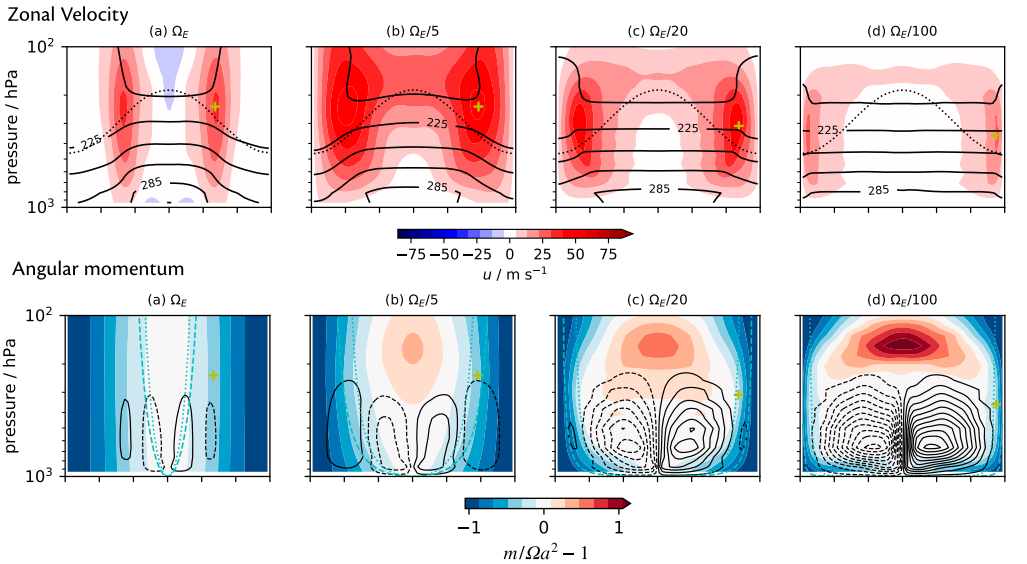

Figure 5. A series of numerical integrations using an idealized General Circulation Model (Isca, [43]) in an Earth-like setting but with the rotation rate varying from that for Earth (Ω_E) to $\Omega_E/100$, as in Colyer & Vallis [44]. The upper row shows zonally averaged zonal velocity (colours) and temperature (contours), and the lower panel shows a normalized excess angular momentum (colours), which is a useful measure of superrotation, and meridional overturning stream function (contours). The horizontal axis is latitude, from −90° to +90°.

latitudes. Given these remarks, two conditions must be satisfied for a significant interaction to occur: (i) the Rossby wave needs to be Doppler shifted eastward by a background flow so its phase speed and frequency match that of the Kelvin wave. (Such an eastward shift can naturally arise if there is an eastward thermal wind in the extratropics. A westward shift of the Kelvin wave is also possible in some circumstances [50].) (ii) The Rossby wave and Kelvin wave should have some physical proximity; otherwise, the interaction will be weak. In practice, this means that the Rossby waves should be generated within a distance of the order of an equatorial deformation radius from the equator. A third, more subtle, requirement arises because Kelvin waves are symmetric across the equator. (Antisymmetric modes, such as Yanai waves, do exist but are less easily excited.) If the RK mode is equatorially symmetric (with $v = 0$ at the equator at all times), then it cannot converge momentum to the equator in the absence of vertical momentum transport. This is because the inviscid zonal momentum equation may be written (using pressure coordinates for convenience) as

$$\frac{\partial u}{\partial t} - (f + \zeta)\, v + \omega \frac{\partial u}{\partial p} = -\frac{\partial}{\partial x}\left(\phi + \frac{1}{2}u^2\right), \tag{3.4}$$

where p is the pressure, ω is the pressure vertical velocity and ϕ is the geopotential. The zonally averaged equation is then

$$\frac{\partial \overline{u}}{\partial t} = \overline{(f + \zeta)\, v} - \overline{\omega \partial_p u}. \tag{3.5}$$

In a model with no vertical variation, the terms involving ω disappear, and the terms involving $\overline{v}$ alone cannot give rise to superrotation (as discussed in §3a). Omitting them, we are left with

$$\frac{\partial \overline{u}}{\partial t} = \overline{v' \zeta'}. \tag{3.6}$$

Downloaded from royalsocietypublishing.org/rsta/article-pdf/doi/10.1098/rsta.2025.0135/6176045/rsta.2025.0135.pdf
by ETH Zurich user
on 23 November 2026

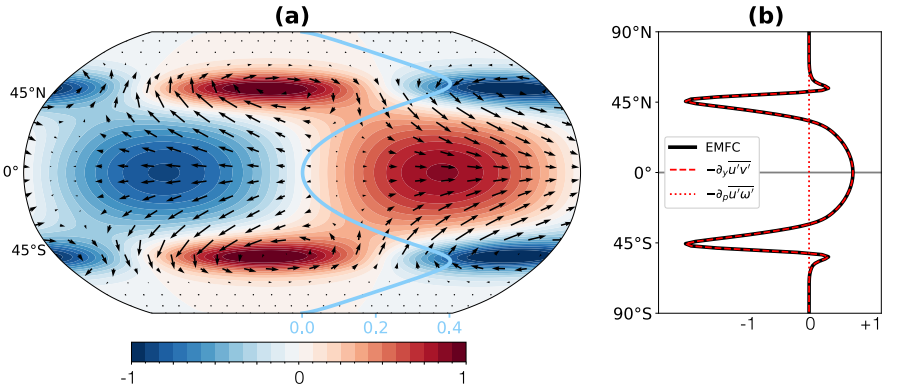

Figure 6. (a) Structure of a Rossby–Kelvin eigenmode in the upper level of a two-level model. Shading shows the geopotential height perturbation, and arrows show the horizontal wind perturbation. This is the most unstable mode arising from the linearization of the primitive equations with a barotropic background state whose zonal wind is shown as a blue line. The bottom light blue scale shows the local Rossby number $U/(2a\Omega)$ of that zonal wind, and the amplitude of the perturbation shown in the colour bar is in arbitrary units. The mode propagates eastward at a speed of $0.4a\Omega$. (b) Eddy momentum flux convergence (black), and its horizontal (dashed red) and vertical (dotted red) components. Figure adapted from Nicolas & Vallis [50].

The term on the right-hand side vanishes if $v' = 0$ at all times. In a single-layer shallow-water model, an essentially similar argument begins by writing the momentum equation as

$$\frac{\partial u}{\partial t} - (f + \zeta)\, v = -\frac{\partial}{\partial x}\left(\phi + \frac{1}{2}u^2\right). \tag{3.7}$$

After zonally averaging, equation (3.6) is again found. The point to be made is that $\overline{v'\zeta'}$, rather than $\partial\overline{u'v'}/\partial y$ alone, is the relevant eddy momentum flux, so that if $v' = 0$ at the equator (for example, because the instability is symmetric across the equator), single-layer models cannot produce superrotation unless vertical momentum transport is parameterized, as inferred by Showman & Polvani [51]. Superrotation in slow rotators is also not well reproduced in a 'one-and-a-half' layer model (i.e. a model with a single moving layer overlying a quiescent layer) even when vertical transport is parametrized [49], and more vertical structure is needed to properly capture it.

The RK instability produces a characteristic pattern that transports zonal momentum equatorward, producing a prograde jet straddling the equator. A sample pattern—an eigenmode of the instability—is illustrated in figure 6, using a two-level primitive equation model, which is perhaps the simplest model that can naturally produce superrotation by this mechanism. The basic state is zonally symmetric, with a pole–equator temperature gradient producing an eastward flow in mid-latitudes (the pale blue line in the figure), Doppler shifting the Rossby waves. The eddy momentum flux produced by the pattern is shown in the right-hand panel, and is such as to produce a prograde equatorial jet. Although it appears from the figure that the horizontal momentum flux convergence is solely responsible for the eddy flux convergence, this is slightly misleading. The eddy flux convergence may also be written as $\overline{v'\zeta'} - \overline{w'\partial_p u'}$ and, for this kind of eigenmode, $v' = 0$ at the equator. Thus, at the equator, the eddy flux convergence involves a correlation between the *vertical* velocity and the vertical shear of the zonal flow, emphasizing the importance of the phase difference, or baroclinicity, in the vertical structure of the zonal flows.

In fully nonlinear integrations, a basic-state zonal wind profile such as that of figure 6 is not externally imposed but naturally appears as a consequence of thermal-wind balance, modified by the action of baroclinic eddies. Slower planetary rotation (or large thermal Rossby number) tends to favour both a wide meridional extent of Kelvin waves and stronger local Rossby number at mid-latitudes. Both effects favour RK instability, and indeed superrotation robustly increases as planetary rotation decreases in such simulations (the parameter dependence is explored in [50]).

Downloaded from royalsocietypublishing.org/rsta/article-pdf/doi/10.1098/rsta.2025.0135/6176045/rsta.2025.0135.pdf
by ETH Zurich user
on 23 November 2026

The importance of nonlinear effects was also noted by Zurita-Gotor & Held [49] and, in a different context, by Lutsko [52]. The production of equatorial superrotation shifts the phase speed of the equatorial Kelvin waves eastward, potentially damping the interaction with the off-equatorial Rossby waves and damping the instability. This leads to an intermittency in the eddy momentum flux producing the superrotation, as found by Mitchell & Vallis [47] and explored by Nicolas & Vallis [50] and Zurita-Gotor *et al.* [53].

(ii) Tidally locked planets

Direct measurements of zonal wind are very difficult to make for exoplanets; however, the phase curve of radiation received from the combined planet and host star system suggests that, at least in some cases, the hottest region is offset from the substellar point (the point on the equator directly below the host star) in the direction of the planetary rotation (as described by Knutson *et al.* [54], and others since). If the offset is owing to advection, then superrotation may be inferred, and this was explored using a shallow-water model by Showman & Polvani [55] and then by Hammond & Pierrehumbert [56], who showed that standing waves are also important.

In a tidally locked planet, the source of heating is stationary and concentrated around the equator, suggesting that the response is likely to be something resembling the Gill pattern ([57]; see figure 7), albeit with parameters more appropriate to a slowly rotating planet. (Matsuno [58] derived a similar pattern using a periodic forcing, and if no differentiation between the two patterns is needed, they are commonly referred to as Matsuno–Gill (MG) patterns.) The basic structure is an equatorial Kelvin mode extending eastward from the heating and two off-equatorial Rossby waves extending westward. The pattern is symmetric across the equator, and therefore, a single-layer model cannot produce superrotation. However, its characteristic chevron shape suggests that with some modification, momentum convergence towards the equator should occur, as with RK instability, and adding vertical structure to the problem does lead to converging eddy momentum fluxes and superrotation [59,60].

The MG pattern produced by solar irradiation on a two-level tidally locked spherical planet is illustrated in figure 7. The lower-layer structure has the canonical chevron-shaped structure, which leads the horizontal flow to converge prograde momentum at the equator. The upper-layer pattern is very different owing to the absence of drag, but prograde momentum flux convergence is carried there vertically from the lower layer. Numerical integrations of the full equations of motion show that, at least in some parameter regimes, superrotation can be produced. If the Rossby number is reasonably small, the superrotation can be traced back to the eddy fluxes produced by the MG model. If the Rossby number is large, a quasi-linear approach is less successful—an exploration of the parameter regime is given in [50]. Superrotation in more complete models —for example multi-layer GCMs (General Circulation Models) with a full radiation scheme and hydrology cycle—also robustly appears, as illustrated in figure 8, where the hot spot is shifted slightly east of the substellar longitude.

However, superrotation does not always arise, and two factors that do affect its appearance are the strength of low-level drag and the optical thickness of the atmosphere, as discussed by Nicolas & Vallis [50]. Drag is important because it affects the phase relation between the lower and upper levels, and hence the crucial vertical transfer of momentum, and without some form of surface drag, superrotation is less likely to occur. Similarly, optical thickness is important because it affects the phase relation between the thermal forcing from the host star and the response.

(c) Superrotation and jets in deep atmospheres

Giant planets, at least those in our Solar System, differ considerably from terrestrial planets in having no clear demarcation between the gaseous atmosphere and a solid planet beneath. The gas

Downloaded from royalsocietypublishing.org/rsta/article-pdf/doi/10.1098/rsta.2025.0135/6176045/rsta.2025.0135.pdf
by ETH Zurich user
on 23 November 2026

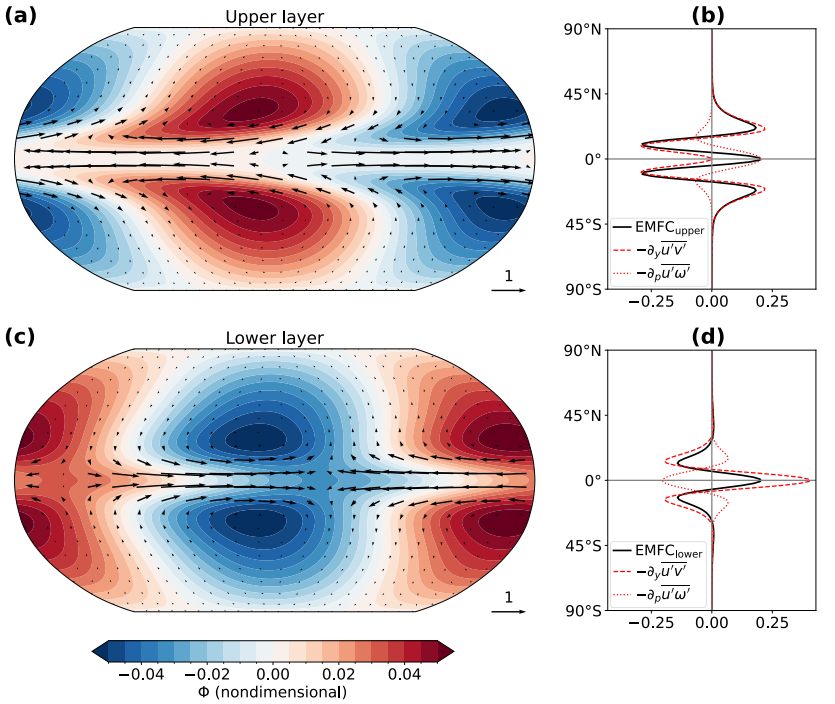

Figure 7. Matsuno–Gill (MG) pattern produced by solar irradiation on a tidally locked spherical planet using a two-level primitive equation model on the sphere, described in Nicolas & Vallis [50]. The left-hand panels show geopotential and horizontal wind perturbations, as in figure 6. The eddy flux convergences shown in the right-hand panels indicate momentum flux convergence at the equator, which leads to superrotation in a time-evolving model.

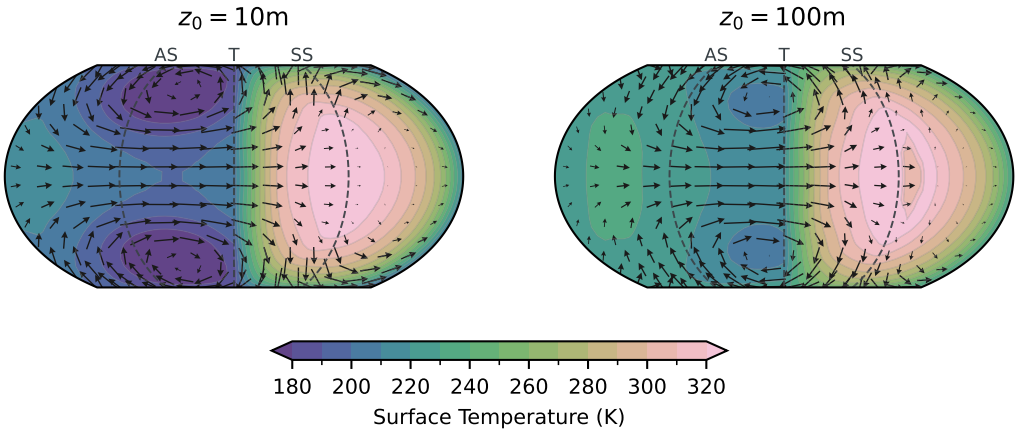

Figure 8. Temperature (colours) and wind (vectors) in two GCM simulations of a moist, Earth-like planet with an active hydrology cycle, tidally locked with a rotation period of about 10 days and inventories of water equivalent to depths of 10 and 100 m. The temperatures are at the surface and the velocity vectors are at 500 hPa. From left to right, the three faint dashed meridional lines are the anti-stellar, terminator and substellar longitudes. Adapted from Williams [61].

giants, Jupiter and Saturn, also superrotate and have multiple extra-tropical zonal jets, whereas the ice giants, Uranus and Neptune, neither superrotate nor have multiple jets.[1] Here, we focus on

[1]The terms 'gas giants' and 'ice giants' are both misnomers, as the respective planets are neither predominantly gaseous nor icy. Nevertheless, the names are embedded in the community.

Downloaded from royalsocietypublishing.org/rsta/article-pdf/doi/10.1098/rsta.2025.0135/6176045/rsta.2025.0135.pdf
by ETH Zurich user
on 23 November 2026

the gas giants, and consider the mechanisms that might give rise to these jets, and we then briefly speculate as to why the jets on the ice giants are quite different.

As noted in the Introduction, there has been something of a debate in the community over the last few decades as to whether the observed jets on Jupiter and Saturn are 'deep' or 'shallow'. The former means that the jets extend into (or originate from) a significant depth in the interior, requiring a full treatment of the Coriolis force with non-hydrostatic equations of motion. Inversions based on gravimetric observations [38] suggest that the jets are aligned with the axis of rotation and extend into the interior about 3000 km in the radial direction, although variations of this depth with latitude are possible (and, in particular, the extra-tropical jets could be shallower). Now, flow in shallow atmospheres feels a β-effect because of the variation of the vertical (i.e. radial, aligned with gravity) component of the rotation vector with latitude. No such effect occurs in the same way in deep flows, but if the planet is rapidly rotating and in a spherical shell, then the first effect causes the topology of any convection cells to be aligned with the rotation vector (the Taylor–Proudman effect), and the geometry of the shell means that the vertical extent (i.e. in the axial direction) of the convection varies with latitude, giving rise to the topographic β-effect (figure 4).

A number of authors have explored these effects, perhaps beginning with Busse [33,34] and with later numerical and theoretical contributions by Julien *et al.* [35], Brummell & Hart [62], Yano *et al.* [63], Busse [64] and others, with Jones *et al.* [65] finding multiple jets in a Brummel-like model applied to Jupiter. A key consideration is the following: if the strong rotation constrains the motion to such a degree that axial variations of the horizontal flow (meaning flow orthogonal to the rotation axis) are small, then some kind of rotating shallow water or quasi-geostrophic approximation may be made. The β-effect arising from the variations of the vertical extent of the flow can in principle give rise to Rossby-like waves, and these in turn can give rise to zonal jets, and possibly a zonostrophic regime, in a manner similar to that for shallow atmospheres. However, the precise way in which this works is unsettled, as is the importance or otherwise of the weather layer atop the convective layer, as we now discuss.

(i) Mechanisms and details

Although a sloping boundary is sufficient to produce a topographic β-effect, the particular way that the boundary slopes may be important for the nature and direction of the jets produced. Specifically, Busse argues that the convex nature of the boundary of the convecting flow is a key aspect of the mechanism, for here the columns tend to spiral outward in the prograde direction, producing a flow with higher angular velocity nearer the outside of the column; i.e. nearer the equator (figure 9). The reverse would occur if the boundary were concave. In this picture, the prograde motion at the equator, seen on Jupiter and Saturn, depends on the tilt of the Taylor-column cross-sections. The mechanism is one of three-dimensional angular momentum transport, involving components both in spherical radius and latitude. Because the equator is further from the rotation axis, in the convex case cylindrically outward angular momentum transport is manifested as a prograde flow in equatorial regions. If for some reason the upper boundary were concave in equatorial regions, then subrotating equatorial flow might be expected, as is seen on Uranus and Neptune, although other mechanisms for subrotation are certainly possible.

Any such jets produced by this or a similar mechanism can be expected to be in good thermal wind balance, given the low Rossby number of the giant planet atmospheres (at least in the Solar System), although the degree to which the temperature gradient shows any alternating pattern will depend on the vertical structure of the jets and how they decay with depth. (The Solar System giants have a weaker meridional temperature gradient than Earth, and a larger rotation rate, so the prograde flow owing to thermal wind balance with the pole–equator temperature gradient alone will be relatively weak compared to the individual jets.)

A Busse-like mechanism is also believed to drive solar differential rotation, for the Sun exhibits a relatively fast equatorial motion [66] and could thus be considered 'superrotating'. Fully three-dimensional, turbulent simulations of angular momentum transport in the stellar context have

Downloaded from royalsocietypublishing.org/rsta/article-pdf/doi/10.1098/rsta.2025.0135/6176045/rsta.2025.0135.pdf
by ETH Zurich user
on 23 November 2026

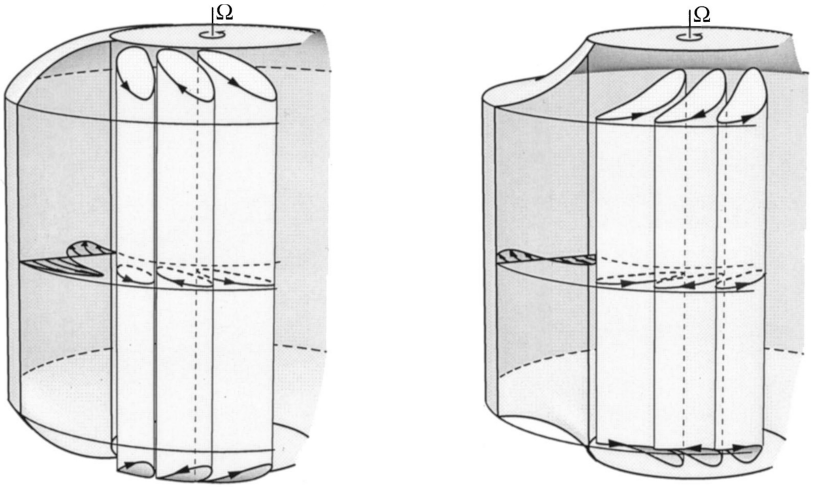

Figure 9. Schematic, from [64], of the influence of curved conical boundaries on the zonal flow. In the convex case, the columns tend to spiral outward in the prograde direction, thus creating a differential rotation with higher angular velocity on the outside than on the inside, with the reverse occurring with concave boundaries.

commonly reproduced solar-like differential rotation [67–71], and fig. 4 of [67] is a schematic of the mechanisms of superrotation not unlike that of figure 9. However, the correspondence between stellar differential rotation and planetary superrotation (with brown dwarfs a useful intermediary) remains to be fully explored.

A seemingly different explanation of the appearance of zonal flows arises from a potential vorticity perspective, if one makes the (perhaps extreme) simplification that the shell of convecting fluid may be treated using the shallow water equations [11,63]. The potential vorticity, Q, in such a system is given by

$$Q = \frac{\zeta^* + 2\Omega}{H}, \tag{3.8}$$

where ζ^* is the axial relative vorticity (i.e. that aligned with the axis of rotation) and H is the depth of the fluid layer in the axial direction, as in figure 4. The rotation rate Ω is constant, but H varies with distance from the axis of rotation, and so with latitude, giving a topographic β-effect. To see this, assume that the Rossby number is small and that variations in H occur on a larger scale than variations in ζ^*. The evolution equation for Q then becomes

$$\frac{DQ}{Dt} \approx \frac{1}{H}\frac{D\zeta^*}{Dt} + 2\Omega\frac{D}{Dt}\left(\frac{1}{H}\right) = \frac{1}{H}\frac{D\zeta^*}{Dt} - \frac{2\Omega}{H^2}v\cdot\nabla H = \frac{1}{H}\left(\frac{D\zeta^*}{Dt} + \beta^* v\right), \tag{3.9}$$

where $\beta^* = -(2\Omega/H)\partial H/\partial y$ and v is the velocity in the y-direction (figure 4). Evidently, β^* is negative outside the tangent cylinder, positive within it.

If the potential vorticity outside the tangent cylinder is homogenized, then a straightforward calculation [11, ch. 13] shows that the zonal flow will be a maximum at the equator. Three-dimensional numerical simulations of convection in deep spherical shells in a giant-planet setting do commonly give rise to prograde motion outside the tangent cylinder, e.g. [72,73]; furthermore, high-resolution simulations run for thousands of rotation periods show partial potential vorticity homogenization accompanying the prograde motion (figure 10). The homogenization is not complete and occurs on the zonally averaged quantity $\overline{Q}$. The variation of the height H with cylindrical radius, and so with latitude, is crucial here; if H is taken to be constant in the evaluation of Q, homogenization of the potential vorticity does not occur. In the extra tropics, simulations of this nature can produce multiple alternating jets, although there is a tendency for the extra-tropical jets to merge and/or seemingly drift poleward over a very long time period [74,75]. The

Downloaded from royalsocietypublishing.org/rsta/article-pdf/doi/10.1098/rsta.2025.0135/6176045/rsta.2025.0135.pdf
by ETH Zurich user
on 23 November 2026

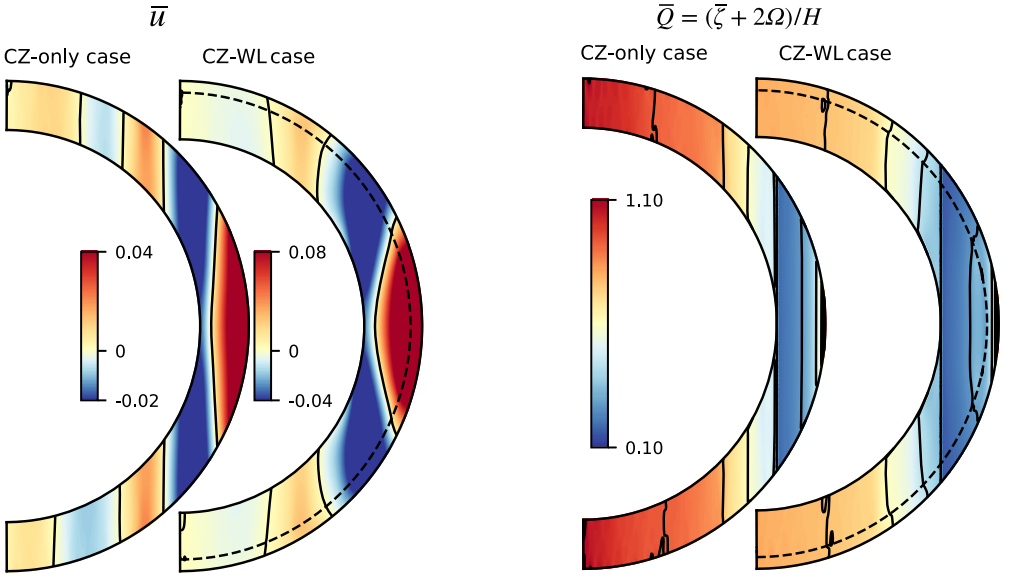

Figure 10. Results from two three-dimensional simulations of the anelastic equations in a spherical, rotating shell forced by heating at the inner boundary and cooling at the top, with Jupiter-like parameters. 'CZ-only' means the simulations have only a convective zone and 'CZ-WL' means a stratified, weather-layer zone is imposed at the top, with the dashed semicircle denoting the base of the weather layer. The two left plots show the zonally-averaged zonal velocity, $\overline{u}$. The two right plots show potential vorticity, defined as $\overline{Q} = (\overline{\zeta^*} + 2\Omega)/H$ (see text and figure 4). $\overline{Q}$ is partially homogenized in the region outside of the tangent cylinder, and a stepped structure is apparent inside the tangent cylinder. Simulations from Matilsky *et al.* [75].

mechanism for this is not fully understood but may be related to the fact that these simulations use a Laplacian viscosity and have insufficient drag to remove energy at large scales, either at the top or bottom of the convective layer, although the origin of any such drag is not known. Relatedly, Rotvig & Jones [76] found multiple jets in simulations with bottom friction but not in simulations with Laplacian viscosity.

The potential-vorticity homogenization mechanism makes no explicit reference to the convexity or concavity of the bounding surface; rather, prograde equatorial motion arises from the homogenization with a negative β-effect, and the relation between the mechanisms is not entirely understood. Fully three-dimensional simulations are expensive and currently prohibit the full exploration of different shapes of bounding surfaces. Two-dimensional simulations do allow one to impose varying types of β-effect, and if a β-effect is imposed that mimics the topographic β-effect of the gas giant planets a prograde, superrotating jet is found in equatorial regions [77]. If the region outside of the tangent cylinder is greater (in meridional extent) than the relevant jet scale (e.g. an appropriate Rhines scale), then multiple jets can be expected to form in that region. This effect can be reproduced in two-dimensional simulations, and there is some evidence for this in figure 10. However, the effect seems not to be present on the gas giants in the Solar System; that is, the superrotating region seems to occupy the full region outside the tangent cylinder. That said, there is some uncertainty as the radial thickness of the convecting shell, and the latitudinal extent of the tangent cylinder is thus not precisely known. Also, Jupiter does exhibit distinct peaks of prograde flow within the equatorial region, perhaps suggesting weaker and possibly shallow alternating jets superimposed on the deeper prograde flow.

(ii) Effects of a weather layer

The visually observed jets in the Solar System gas giants reside in an upper, stratified, weather layer, but gravimetric inversions suggest that the jets extend well below that layer. Thus, some

Downloaded from royalsocietypublishing.org/rsta/article-pdf/doi/10.1098/rsta.2025.0135/6176045/rsta.2025.0135.pdf
by ETH Zurich user
on 23 November 2026

interaction between the convective and stratified layers is expected. If the solar differential heating in the weather layer gives rise to baroclinic instability, and thence geostrophic turbulence in a differentially rotating background state, then jets can be excited there independently of the convectively induced ones, although there are less certain mechanisms for the production of superrotation. (These possibilities are discussed more in §4).

In the absence of baroclinic instability in the weather layer, three-dimensional simulations by Matilsky *et al.* [75] of a stratified layer above a convective layer suggest that one significant effect of the weather layer is to tilt the flow structures so that zonal flow contours become radially aligned rather than axially aligned (figure 10). The shallowness of the weather layer and the low density of the fluid within it suggest that their gravitational signature of this effect will be weak, and so this result is not inconsistent with observations. Even if the tilting occurs mainly inside the weather layer, it does have an effect deeper into the convective layer, although the convective cells do remain largely aligned with the rotation axis. The region in the weather layer is convectively stable (by construction of the model), yet the convective overshoot enables the jets to penetrate well into that layer. All things considered, the very robust production of convectively forced jets, taken with the results from inversions, does suggest that deep convection has a significant influence in the weather layer and may be the primary cause of the observed jets. This said, and given that simulations of the weather layer *without* any deep underlying convection can produce zonal jets, it should be said that aspects of the dynamics remain unsettled, as we now discuss.

4. Uncertainties, realities and open questions

Various mechanisms for jet production and superrotation are now becoming established, but it is less clear which mechanism applies, and under what circumstances, in the different planetary atmospheres. On Earth-like atmospheres (and in particular on Earth), the extra-tropical eddy-driven jets arise from the action of Rossby-like waves, superimposed on a broader prograde flow arising from thermal wind balance in an atmosphere with a pole–equator temperature gradient. The processes in Earth's atmosphere are certainly more complicated than figure 1 implies, with baroclinic instability, shear of the background flow, the influence of the subtropical jet and fully nonlinear effects all playing a role. Furthermore, even with the detailed observations and reanalysis (i.e. state estimates) we have for Earth, direct unambiguous evidence of Rossby wave activity is hard to come by. Nevertheless, a β-effect caused by a potential vorticity gradient in a shallow, stratified atmosphere almost certainly plays a role in the jet-producing mechanism.

In slowly rotating terrestrial atmospheres, simulations show that the Rossby–Kelvin instability provides a robust mechanism for superrotation. We have no clear, direct observations of the instability in either of the planetary bodies (namely, Titan and Venus) in the Solar System for which the mechanism seems likely to apply. Furthermore, Venus is strongly affected by tidal forces, and their effect on the vertical transport of momentum is likely to be important. Numerical simulations of Venus vary widely in their results, making it difficult to determine what the precise mechanism is, or whether there is a single dominant one.

In tidally locked shallow atmospheres, a mechanism that involves the interaction of Rossby and Kelvin modes also seems likely to be important in producing superrotation, but direct evidence is unobtainable and will be for some time. Indirect evidence of superrotation, such as the degree of offset of the hot spot relative to the substellar point, or possibly a measure of the meridional temperature gradient, may nevertheless give some guidance. The presence of superrotation also depends on the physical properties of the atmosphere, and it seems possible that, if and when confidence in numerical simulations is established, the simulations and theory can be used to help characterize the physical properties of the planetary atmosphere. A number of simulations have highlighted the importance of drag in producing superrotation, and this brings in a major uncertainty: many tidally locked planets are gas giants (although some are super-Earths), and gas giants

Downloaded from royalsocietypublishing.org/rsta/article-pdf/doi/10.1098/rsta.2025.0135/6176045/rsta.2025.0135.pdf
by ETH Zurich user
on 23 November 2026

have no solid layer that might provide such a drag. Also, our theories regarding the response to the thermal forcing are largely based around shallow atmospheres. This may partially be justified as the solar forcing greatly exceeds the internal thermal forcing (on tidally locked planets), but the influence of the planetary interior remains largely unexplored.

A number of outstanding issues remain regarding the giant planets in the Solar System, with a primary example being the nature of the interaction between the stratified weather layer and the deeper convective layer. It seems very likely that convective motion in the interior does produce zonal flows, and that these manifest themselves in the weather layer, but the degree to which the weather layer can produce jets *independently* is not known with any certainty. Many simulations of the weather layer alone do produce jets with a similar character to that of the gas giants (beginning with [78] and more recently [79]), although the production of superrotation is less common. The kind of superrotation that is seen on Jupiter and Saturn is robustly reproduced in three-dimensional simulations as a consequence of a rapidly rotating convection in the presence of negative β-effect, and two-dimensional simulations show a similar effect if the convection is parametrized. Although that effect is very natural, simulations of Jupiter's atmosphere with shallow-atmosphere or shallow-water models can also give rise to superrotation (e.g. [36,37,79]). The results depend on the parameters chosen, in particular those representing mechanical drag, thermal damping and moist effects; however, this does not preclude Saturn and Jupiter being in a parameter regime where superrotation *is* produced by effects in the weather layer, with deeper jets either being a downward extension of the weather layer jets or independent of them. The zonal flows on the sub-ice-layer global oceans of the icy moons, such as Europa and Enceladus, may well resemble that of the gas giants, in that it is convectively forced from below. If so, superrotation seems likely, since the geometry, with regions inside and outside a tangent cylinder, is similar, and some simulations reproduce such flow e.g. [80]. However, complications abound—the effects of salinity, the possible internal heating of the water itself and an uneven upper surface—and observations are very limited. An observationally verified understanding of the flows on such bodies seems unlikely to occur in the foreseeable future, but the prospect that they may be incubators of life means interest in them will remain.

The lack of multiple jets on the ice giants (Uranus and Neptune) and their lack of superrotation suggest that their dynamics are quite different from those of the gas giants, and various suggestions have been made as to what the essential difference is (e.g. [77,81,82]). The internal heat flux of Neptune is an order of magnitude smaller than that of the gas giants, and that of Uranus much smaller still, suggesting that the small-scale convective forcing that might stochastically excite multiple jets is weak, yet the zonal flow itself is strong. If the main forcing of the flow is at a large scale (either internal or from solar forcing) and the flow is shallow, then subrotating equatorial flow with broad prograde flows in higher latitudes is more likely than superrotating flow, certainly in the absence of any mechanism generating Rossby waves at the equator. However, the internal structures of Uranus and Neptune are comparatively poorly known [83], and in particular, little is certain about the depth of the convective layer (assuming such a layer exists) or whether there is any meaningful concept of there being different regions inside and outside of a tangent cylinder. Evidently, we are at the early stages of understanding how the flow on the ice giants is maintained, and we will not discuss them further in this article.

5. Conclusion

Let us conclude by summarizing what we can say, with some confidence, about jets and superrotation in planetary atmospheres. On rapidly rotating planets (i.e. $Ro < 1$) with shallow atmospheres, of which we take Earth to be such, one or more jets in mid-latitudes can be formed by quasi-two-dimensional mechanisms involving turbulence and/or Rossby waves, as adumbrated by Thompson [6], Rhines [12], Vallis & Maltrud [13] and others since. There are natural mechanisms for the production of the required waves and eddy flow—baroclinic instability is one—and on Earth the resulting mid-latitude jet is commonly known as the eddy-driven jet. This jet is superimposed on

Downloaded from royalsocietypublishing.org/rsta/article-pdf/doi/10.1098/rsta.2025.0135/6176045/rsta.2025.0135.pdf
by ETH Zurich user
on 23 November 2026

a broad prograde flow that is in thermal wind balance with the meridional temperature gradient. Equatorial superrotation can also be produced by Rossby waves, and although the mechanisms for equatorial Rossby wave production on giant planets are less well established, this remains a candidate mechanism for the production of superrotation on Jupiter and Saturn.

Multiple mid-latitude jets can be produced by such mechanisms, and the rapidly rotating gas giant planets in our Solar System (i.e. Jupiter and Saturn, for which the Rossby number is much smaller than in Earth's atmosphere) do exhibit multiple jets in their mid-latitudes, as well as equatorial superrotation. However, inversions of gravitational data suggest that the jets extend, or originate from, a few thousands of kilometres deep in the interior on Jupiter and even deeper on Saturn, certainly in lower latitudes. The interior heating in these planets is likely to give rise to convection, and hence to flow that is three-dimensional in nature. However, in the presence of rapid rotation in a spherical shell, the flow can be approximately described by equations that are quasi-two-dimensional, resembling the familiar quasi-geostrophic equations. The geometry (in particular the sloping boundaries at the top and bottom of the shell) then gives rise to a topographic β-effect, which leads to the production of zonal jets *and* superrotation. These mechanisms are quite robust and have been reproduced in a number of numerical simulations. The effect of a stably stratified weather layer lying above the convection means that truly shallow mechanisms cannot be ruled out as having an important effect on the observed jets, especially in mid-latitudes and high latitudes. A reasonable conjecture, consistent with observations and numerical simulations, is that on rapidly rotating gas giants, equatorial superrotation is produced by predominantly deep dynamics, whereas in mid-latitudes shallow, weather-layer dynamics play an important and possibly essential role.

In slowly rotating shallow atmospheres, an instability involving the interaction of Rossby and Kelvin waves provides a robust mechanism for the production of prograde flow at the equator, and this is a candidate mechanism for the production of superrotation on Titan and Venus. (This mechanism may not be the whole story; for example, on Venus thermal tides may play a role.) On tidally locked planets, the interaction of Rossby and Kelvin modes—now directly forced by stellar insolation—also provides a mechanism for superrotation. In numerical simulations, the mechanism is found to be robust, although it does not always produce superrotation and not all tidally locked planets can be expected to superrotate. Two other caveats are that direct observational verification of the mechanism is obviously hard to come by, and many tidally locked planets are gas giants with a potentially deep structure. Little is known about the internal dynamics of slowly rotating deep planetary atmospheres, tidally locked or otherwise.

Data accessibility. This article has no additional data.

Declaration of AI use. We have not used AI-assisted technologies in creating this article.

Authors' contributions. G.V.: conceptualization, investigation, writing—original draft, writing—review and editing; L.M.: investigation, writing—review and editing; Q.N.: investigation, writing—review and editing.

All authors gave final approval for publication and agreed to be held accountable for the work performed therein.

Conflict of interest declaration. We declare we have no competing interests.

Funding. No funding has been received for this article.

Acknowledgements. The authors would like to acknowledge discussions with Matt Browning, Nicholas Brummel, Glenn Flierl, Wanying Kang, Neil Lewis, Jonathan Mitchell, Heng Quan, Adrian Van Kan and Yaoxuan Zeng.
For the purpose of open access, the authors have applied a Creative Commons Attribution (CC BY) license to any Author Accepted Manuscript version arising from this submission.

References

1. Imamura T, Mitchell J, Lebonnois S, Kaspi Y, Showman AP, Korablev O. 2020 Superrotation in planetary atmospheres. *Space Sci. Rev.* **216**, 87. (doi:10.1007/s11214-020-00703-9)
2. Read PL, Lebonnois S. 2018 Superrotation on Venus, on Titan, and elsewhere. *Ann. Rev. Earth Plan. Sci.* **46**, 175–202. (doi:10.1146/annurev-earth-082517-010137)

Downloaded from royalsocietypublishing.org/rsta/article-pdf/doi/10.1098/rsta.2025.0135/6176045/rsta.2025.0135.pdf
by ETH Zurich user
on 23 November 2026

3. Pierrehumbert RT, Hammond M. 2019 Atmospheric circulation of tide-locked exoplanets. *Ann. Rev. Fluid Mech.* **51**, 275–303. (doi:10.1146/annurev-fluid-010518-040516)
4. Read PL. 2024 The dynamics of Jupiter's and Saturn's weather layers: a synthesis after Cassini and Juno. *Ann. Rev. Fluid Mech.* **56**, 271–293. (doi:10.1146/annurev-fluid-121021-040058)
5. Galperin B, Read PL. 2019 *Zonal jets: phenomenology, genesis, and physics*. Cambridge, UK: Cambridge University Press.
6. Thompson RORY. 1971 Why there is an intense eastward current in the North Atlantic but not in the South Atlantic. *J. Phys. Oceanogr.* **1**, 235–237. (doi:10.117/1520-0485(1971)001<0235:wtiaie>2.0.co;2)
7. Thompson RORY. 1980 A prograde jet driven by Rossby waves. *J. Atmos. Sci.* **37**, 1216–1226. (doi:10.1175/1520-0469(1980)037<1216:APJDBR>2.0.CO;2)
8. Dickinson RE. 1969 Theory of planetary wave-zonal flow interaction. *J. Atmos. Sci.* **26**, 73–81. (doi:10.1175/1520-0469(1969)026<0073:TOPWZF>2.0.CO;2)
9. Vallis GK. 2017 *Atmospheric and oceanic fluid dynamics: fundamentals and large-scale circulation.* Cambridge, UK: Cambridge University Press.
10. Marshall J, Plumb RA. 2008 *Atmosphere, ocean and climate dynamics: an introductory text*. Amsterdam, The Netherlands: Academic Press.
11. Vallis GK. 2019 *Essentials of atmospheric and oceanic dynamics*. Cambridge, UK: Cambridge University Press.
12. Rhines PB. 1975 Waves and turbulence on a β-plane. *J. Fluid Mech.* **69**, 417–443. (doi:10.1017/s0022112075001504)
13. Vallis GK, Maltrud ME. 1993 Generation of mean flows and jets on a beta plane and over topography. *J. Phys. Oceanogr.* **23**, 1346–1362. (doi:10.1175/1520-0485(1993)023<1346:GOMFAJ>2.0.CO;2)
14. Newell AC. 1969 Rossby wave packet interactions. *J. Fluid Mech.* **35**, 255–271. (doi:10.1017/s0022112069001108)
15. Galperin B, Nakano H, Huang HP, Sukoriansky S. 2004 The ubiquitous zonal jets in the atmospheres of giant planets and Earth's oceans. *Geophys. Res. Lett.* **31**, 2004GL019691. (doi:10.1029/2004gl019691)
16. Sukoriansky S, Galperin B, Dikovskaya N. 2002 Universal spectrum of two-dimensional turbulence on a rotating sphere and some basic features of atmospheric circulation on giant planets. *Phys. Rev. Lett.* **89**, 124501. (doi:10.1103/physrevlett.89.124501)
17. Kraichnan R. 1967 Inertial ranges in two-dimensional turbulence. *Phys. Fluids* **10**, 1417–1423. (doi:10.1063/1.1762301)
18. Chai J, Jansen M, Vallis GK. 2016 Equilibration of a baroclinic planetary atmosphere toward the limit of vanishing bottom friction. *J. Atmos. Sci.* **73**, 3249–3272. (doi:10.1175/JAS-D-15-0329.1)
19. Rhines PB, Young WR. 1982 Homogenization of potential vorticity in planetary gyres. *J. Fluid Mech.* **122**, 347–367. (doi:10.1017/s0022112082002250)
20. Marcus PS. 1993 Jupiter's great red spot and other vortices. *Ann. Rev. Astron. Astrophys.* **31**, 523–573. (doi:10.1146/annurev.aa.31.090193.002515)
21. Marcus PS, Shetty S. 2011 Jupiter's zonal winds: are they bands of homogenized potential vorticity organized as a monotonic staircase? *Phil. Trans. R. Soc. A* **369**, 771–795. (doi:10.1098/rsta.2010.0299)
22. Dritschel D, McIntyre M. 2008 Multiple jets as PV staircases: the Phillips effect and the resilience of Eddy-transport barriers. *J. Atmos. Sci.* **65**, 855–874. (doi:10.1175/2007jas2227.1)
23. Scott RK, Dritschel DG. 2012 The structure of zonal jets in geostrophic turbulence. *J. Fluid Mech.* **711**, 576–598. (doi:10.1017/jfm.2012.410)
24. Phillips OM. 1972 Turbulence in a strongly stratified fluid—is it unstable? *Deep Sea Res. Oceanogr. Abstr.* **19**, 79–81. (doi:10.1016/0011-7471(72)90074-5)
25. Posmentier ES. 1977 The generation of salinity finestructure by vertical diffusion. *J. Phys. Oceanogr.* **7**, 298–300. (doi:10.1175/1520-0485(1977)007<0298:tgosfb>2.0.co;2)
26. Cabanes S, Espa S, Galperin B, Young RM, Read PL. 2020 Revealing the intensity of turbulent energy transfer in planetary atmospheres. *Geophys. Res. Lett.* **47**, e2020GL088685. (doi:10.1029/2020gl088685)
27. Thorpe SA. 2005 *The turbulent ocean*. Cambridge, UK: Cambridge University Press.
28. Tait RI, Howe MR. 1968 Some observations of thermo-haline stratification in the deep ocean. *Deep Sea Res. Oceanogr. Abstr.* **15**, 278–280. (doi:10.1016/0011-7471(68)90005-3)

Downloaded from royalsocietypublishing.org/rsta/article-pdf/doi/10.1098/rsta.2025.0135/6176045/rsta.2025.0135.pdf
by ETH Zurich user
on 23 November 2026

29. Charney JG. 1971 Geostrophic turbulence. *J. Atmos. Sci.* **28**, 1087–1095. (doi:10.1175/1520-0469(1971)028<1087:gt>2.0.co;2)
30. Salmon R. 1980 Baroclinic instability and geostrophic turbulence. *Geophys. Astrophys. Fluid Dyn.* **15**, 167–211. (doi:10.1080/03091928008241178)
31. Gupta P *et al*. 2022 Jupiter's temperature structure: a reassessment of the voyager radio occultation measurements. *Plan. Sci. J.* **3**, 159. (doi:10.3847/PSJ/ac6956)
32. Lindal GF *et al*. 1981 The atmosphere of Jupiter: an analysis of the voyager radio occultation measurements. *J. Geophys. Res.* **86**, 8721–8727. (doi:10.1029/ja086ia10p08721)
33. Busse FH. 1970 Thermal instabilities in rapidly rotating systems. *J. Fluid Mech.* **44**, 441–460. (doi:10.1017/s0022112070001921)
34. Busse FH. 1976 A simple model of convection in the Jovian atmosphere. *Icarus* **29**, 255–260. (doi:10.1016/0019-1035(76)90053-1)
35. Julien K, Knobloch E, Milliff R, Werne J. 2006 Generalized quasi-geostrophy for spatially anisotropic rotationally constrained flows. *J. Fluid Mech.* **555**, 233–274. (doi:10.1017/s0022112006008949)
36. Schneider T, Liu J. 2009 Formation of jets and equatorial superrotation on Jupiter. *J. Atmos. Sci.* **66**, 579–601. (doi:10.1175/2008jas2798.1)
37. Lian Y, Showman AP. 2010 Generation of equatorial jets by large-scale latent heating on the giant planets. *Icarus* **207**, 373–393. (doi:10.1016/j.icarus.2009.10.006)
38. Kaspi Y *et al*. 2018 Jupiter's atmospheric jet streams extend thousands of kilometres deep. *Nature* **555**, 223–226. (doi:10.1038/nature25793)
39. Galanti E, Kaspi Y, Miguel Y, Guillot T, Durante D, Racioppa P, Iess L. 2019 Saturn's deep atmospheric flows revealed by the Cassini grand finale gravity measurements. *Geophys. Res. Lett.* **46**, 616–624. (doi:10.1029/2018gl078087)
40. Hide R. 1969 Dynamics of the atmospheres of major planets with an appendix on the viscous boundary layer at the rigid boundary surface of an electrically-conducting rotating fluid in the presence of a magnetic field. *J. Atmos. Sci.* **26**, 841–853. (doi:10.1175/1520-0469(1969)026<0841:DOTAOT>2.0.CO;2)
41. Gierasch PJ. 1975 Meridional circulation and the maintenance of the venus atmospheric rotation. *J. Atmos. Sci.* **32**, 1038–1044. (doi:10.1175/1520-0469(1975)032<1038:mcatmo>2.0.co;2)
42. Sukoriansky S, Galperin B, Chekhlov A. 1999 Large scale drag representation in simulations of two-dimensional turbulence. *Phys. Fluids* **11**, 3043–3053. (doi:10.1063/1.870163)
43. Vallis GK *et al*. 2018 Isca, v1. 0: a framework for the global modelling of the atmospheres of Earth and other planets at varying levels of complexity. *Geosci. Model Dev.* **11**, 843–859. (doi:10.5194/gmd-11-843-2018)
44. Colyer GJ, Vallis GK. 2019 Zonal-mean atmospheric dynamics of slowly rotating terrestrial planets. *J. Atmos. Sci.* **76**, 1397-1418. (doi:10.1175/JAS-D-18-0180.1)
45. Iga S-i, Matsuda Y. 2005 Shear instability in a shallow water model with implications for the Venus atmosphere. *J. Atmos. Sci.* **62**, 2514–2527. (doi:10.1175/jas3484.1)
46. Wang P, Mitchell JL. 2014 Planetary ageostrophic instability leads to superrotation. *Geophys. Res. Lett.* **41**, 4118–4126. (doi:10.1002/2014GL060345)
47. Mitchell JL, Vallis GK. 2010 The transition to superrotation in terrestrial atmospheres. *J. Geophys. Res. (Planets)* **115**, E12008. (doi:10.1029/2010JE003587)
48. Potter SF, Vallis GK, Mitchell JL. 2014 Spontaneous superrotation and the role of kelvin waves in an idealized dry GCM. *J. Atmos. Sci.* **71**, 596–614. (doi:10.1175/jas-d-13-0150.1)
49. Zurita-Gotor P, Held IM. 2018 The finite-amplitude evolution of mixed Kelvin–Rossby wave instability and equatorial superrotation in a shallow-water model and an idealized GCM. *J. Atmos. Sci.* **75**, 2299–2316. (doi:10.1175/jas-d-17-0386.1)
50. Nicolas Q, Vallis GK. 2026 Mechanisms of superrotation in slowly-rotating and tidally-locked planets. *Plan. Sci. J.* **7**, 98. (doi:10.3847/psj/ae5c96)
51. Showman AP, Polvani LM. 2010 The Matsuno–Gill model and equatorial superrotation. *Geophys. Res. Lett.* **37**, L18811. (doi:10.1029/2010gl044343)
52. Lutsko NJ. 2018 The response of an idealized atmosphere to localized tropical heating: superrotation and the breakdown of linear theory. *J. Atmos. Sci.* **75**, 3–20. (doi:10.1175/jas-d-17-0192.1)
53. Zurita-Gotor P, Anaya-Benlliure Á, Held IM. 2022 The sensitivity of superrotation to the latitude of baroclinic forcing in a terrestrial dry dynamical core. *J. Atmos. Sci.* **79**, 1311–1323. (doi:10.1175/jas-d-21-0269.1)

Downloaded from royalsocietypublishing.org/rsta/article-pdf/doi/10.1098/rsta.2025.0135/6176045/rsta.2025.0135.pdf
by ETH Zurich user
on 23 November 2026

54. Knutson HA, Charbonneau D, Allen LE, Fortney JJ, Agol E, Cowan NB, Showman AP, Cooper CS, Megeath ST. 2007 A map of the day–night contrast of the extrasolar planet HD 189733b. *Nature* **447**, 183–186. (doi:10.1038/nature05782)
55. Showman AP, Polvani LM. 2011 Equatorial superrotation on tidally-locked exoplanets. *Astrophys. J* **738**, 71. (doi:10.1088/0004-637x/738/1/71)
56. Hammond M, Pierrehumbert RT. 2018 Wave-mean flow interactions in the atmospheric circulation of tidally locked planets. *Astrophys. J* **869**, 65. (doi:10.3847/1538-4357/aaec03)
57. Gill AE. 1980 Some simple solutions for heat-induced tropical circulation. *Quart. J. Roy. Meteor. Soc.* **106**, 447–462. (doi:10.1002/qj.49710644905)
58. Matsuno T. 1966 Quasi-geostrophic motions in the equatorial area. *J. Meteorol. Soc. Jpn.* **44**, 25–43. (doi:10.2151/jmsj1965.44.1_25)
59. Tsai SM, Dobbs-Dixon I, Gu PG. 2014 Three-dimensional structures of equatorial waves and the resulting super-rotation in the atmosphere of a tidally locked hot Jupiter. *Astrophys. J.* **793**, 141. (doi:10.1088/0004-637x/793/2/141)
60. Hammond M, Tsai SM, Pierrehumbert RT. 2020 The equatorial jet speed on tidally locked planets. I. Terrestrial planets. *Astrophys. J.* **901**, 78. (doi:10.3847/1538-4357/abb08b)
61. Williams D. 2025 *Circulation of moist planetary atmospheres*. PhD thesis, University of Exeter, UK.
62. Brummell NH, Hart J. 1993 High Rayleigh number β-convection. *Geophys. Astrophys. Fluid Dyn.* **68**, 85–114. (doi:10.1080/03091929308203563)
63. Yano JI, Talagrand O, Drossart P. 2005 Deep two-dimensional turbulence: an idealized model for atmospheric jets of the giant outer planets. *Geophys. Astrophys. Fluid Dyn.* **99**, 137–150. (doi:10.1080/03091920412331336398)
64. Busse FH. 2002 Convective flows in rapidly rotating spheres and their dynamo action. *Phys. Fluids* **14**, 1301–1314. (doi:10.1063/1.1455626)
65. Jones C, Rotvig J, Abdulrahman A. 2003 Multiple jets and zonal flow on Jupiter. *Geophys. Res. Lett.* **30**, 1731. (doi:10.1029/2003gl016980)
66. Howe R. 2009 Solar interior rotation and its variation. *Living Rev. Sol. Phys.* **6**, 1. (doi:10.12942/lrsp-2009-1)
67. Gilman PA. 1983 Dynamically consistent nonlinear dynamos driven by convection in a rotating spherical shell. II. Dynamos with cycles and strong feedbacks. *Astro. J. Suppl.* **53**, 243–268. (doi:10.1086/190891)
68. Brun AS, Toomre J. 2002 Turbulent convection under the influence of rotation: sustaining a strong differential rotation. *Astrophys. J.* **570**, 865–885. (doi:10.1086/339228)
69. Matilsky LI, Hindman BW, Toomre J. 2019 The role of downflows in establishing solar near-surface shear. *Astrophys. J.* **871**, 217. (doi:10.3847/1538-4357/aaf647)
70. Matilsky LI, Hindman BW, Toomre J. 2020 Revisiting the Sun's strong differential rotation along radial lines. *Astrophys. J.* **898**, 111. (doi:10.3847/1538-4357/ab9ca0)
71. Camisassa ME, Featherstone NA. 2022 Solar-like to antisolar differential rotation: a geometric interpretation. *Astrophys. J.* **938**, 65. (doi:10.3847/1538-4357/ac879f)
72. Heimpel M, Aurnou J. 2007 Turbulent convection in rapidly rotating spherical shells: a model for equatorial and high latitude jets on Jupiter and Saturn. *Icarus* **187**, 540–557. (doi:10.1016/j.icarus.2006.10.023)
73. Wulff PN, Dietrich W, Christensen UR, Wicht J. 2022 Zonal winds in the gas planets driven by convection above a stably stratified layer. *Mon. Not. Roy. Astron. Soc.* **517**, 5584–5593. (doi:10.1093/mnras/stac3045)
74. Takehiro Si, Sasaki Y, Ishioka K, Enomoto T, Nakajima K, Hayashi YY. 2024 Asymptotic profiles of mean zonal flows generated by thermal convection of Boussinesq fluid in a rapidly rotating thin spherical shell. *Icarus* **420**, 116154. (doi:10.1016/j.icarus.2024.116154)
75. Matilsky LI, Vallis GK, Browning MK, Brummell NH. 2026 Superrotation and jet migration in simulations of giant planet atmospheres. *Plan. Sci. J.* (in press) arXiv:2605.23307. (doi:10.48550/arXiv.2605.23307)
76. Rotvig J, Jones CA. 2006 Multiple jets and bursting in the rapidly rotating convecting two-dimensional annulus model with nearly plane-parallel boundaries. *J. Fluid Mech.* **567**, 117–140. (doi:10.1017/s0022112006002254)
77. Zeng Y, Kang W, Flierl GR, Vallis GK. 2026. Influence of Penetration Depth on Jets on Giant Planets: Equatorial Jet Direction, Jet Numbers, and Jet Energy Fraction. Planet. Sci. J. 7(6), 149. doi:10.3847/psj/ae6da7

Downloaded from royalsocietypublishing.org/rsta/article-pdf/doi/10.1098/rsta.2025.0135/6176045/rsta.2025.0135.pdf
by ETH Zurich user
on 23 November 2026

78. Williams GP. 1978 Planetary circulations: 1. Barotropic representation of Jovian and terrestrial turbulence. *J. Atmos. Sci.* **35**, 1399–1426. (doi:10.1175/1520-0469(1978)035<1399:pcbroj>2.0.co;2)
79. Boissinot A, Spiga A, Guerlet S, Cabanes S, Bardet D. 2024 Global climate modeling of the Jupiter troposphere and effect of dry and moist convection on jets. *Astron. Astrophys.* **687**, A274. (doi:10.1051/0004-6361/202245220)
80. Bire S, Kang W, Ramadhan A, Campin JM, Marshall J. 2022 Exploring ocean circulation on icy moons heated from below. *J. Geophys. Res. (Planets)* **127**, e07025. (doi:10.1029/2021je007025)
81. Liu J, Schneider T. 2010 Mechanisms of jet formation on the giant planets. *J. Atmos. Sci.* **67**, 3652–3672. (doi:10.1175/2010jas3492.1)
82. Duer-Milner K, Gavriel N, Galanti E, Tziperman E, Kaspi Y. 2025 From gas to ice giants: a unified mechanism for equatorial jets. *Sci. Adv.* **11**, eads8899. (doi:10.1126/sciadv.ads8899)
83. Helled R, Fortney JJ. 2020 The interiors of Uranus and Neptune: current understanding and open questions. *Phil. Trans. R. Soc. A.* **378**, 20190474. (doi:10.1098/rsta.2019.0474)

Downloaded from royalsocietypublishing.org/rsta/article-pdf/doi/10.1098/rsta.2025.0135/6176045/rsta.2025.0135.pdf
by ETH Zurich user
on 23 November 2026